University of Nebraska Medical Center

DigitalCommons@UNMC

Journal Articles: Biochemistry & Molecular Biology

Biochemistry & Molecular Biology

miR-25 targets TNF-related apoptosis inducing ligand (TRAIL) death receptor-4 and promotes apoptosis resistance in cholangiocarcinoma.

Nataliya Razumilava
Mayo Clinic

Steve F. Bronk
Mayo Clinic

Rory L. Smoot
Mayo Clinic

Christian D. Fingas
Mayo Clinic

Nathan W. Werneburg
Mayo Clinic

Follow this and additional works at: https://digitalcommons.unmc.edu/com_bio_articles
See next page for additional authors
Part of the Medical Biochemistry Commons, and the Medical Molecular Biology Commons

Recommended Citation

Authors

Nataliya Razumilava, Steve F. Bronk, Rory L. Smoot, Christian D. Fingas, Nathan W. Werneburg, Lewis R. Roberts, and Justin L. Mott

miR-25 Targets TRAIL Death Receptor-4 and Promotes Apoptosis Resistance in Cholangiocarcinoma

Nataliya Razumilava, **Steve F. Bronk**, **Rory L. Smoot**, **Christian D. Fingas**, **Nathan W. Werneburg**, **Lewis R. Roberts**, and **Justin L. Mott**
Division of Gastroenterology and Hepatology, Mayo Clinic, 200 First Street SW, Rochester, MN, 55905, USA.

Abstract

It has been established that microRNA expression and function contribute to phenotypic features of malignant cells, including resistance to apoptosis. While targets and functional roles for a number of microRNAs have been described in cholangiocarcinoma, many additional microRNAs dysregulated in this tumor have not been assigned functional roles. In this study, we identify elevated miR-25 expression in malignant cholangiocarcinoma cell lines as well as patient samples. In cultured cells, treatment with the Smoothened inhibitor, cyclopamine, reduced miR-25 expression, suggesting Hedgehog signaling stimulates miR-25 production. Functionally, miR-25 was shown to protect cells against TNF-Related Apoptosis-Inducing Ligand (TRAIL)-induced apoptosis. Correspondingly, antagonism of miR-25 in culture sensitized cells to apoptotic death. Computational analysis identified the TRAIL Death Receptor-4 (DR4) as a potential novel miR-25 target, and this prediction was confirmed by immunoblot, cell staining, and reporter assays.

Conclusion—These data implicate elevated miR-25 levels in the control of tumor cell apoptosis in cholangiocarcinoma. The identification of the novel miR-25 target DR4 provides a mechanism by which miR-25 contributes to evasion of TRIAL-induced cholangiocarcinoma apoptosis.

MicroRNA expression is altered in a variety of human cancers, with some microRNAs exhibiting increased expression levels and others reduced amounts compared to non tumor samples (1). Functionally, microRNAs contribute to many processes, including oncogenesis, angiogenesis, cell death, and metastasis. Thus, the control of microRNA levels in cancer cells, as well as their particular protein targets, is an active area of investigation.

Among the microRNAs known to be dysregulated in disease states, miR-25 is expressed at altered levels in a number of cancers. miR-25 is 22 nucleotides in length, hosted by the minichromosome maintenance protein-7 (*MCM7*) gene, and transcribed as part of the mir-106b~25 polycistron. Examples of miR-25 dysregulation include its upregulation in pediatric brain tumors of multiple histological classifications (2), prostate carcinoma (3), gastric adenocarcinoma (4), and epidermal growth factor receptor-positive lung adenocarcinoma (5). In the liver, miR-25 is elevated in hepatocellular carcinoma cell lines (6, 7) and human hepatocellular carcinoma samples (8, 9), and was among the microRNAs shown to be overexpressed in intrahepatic cholangiocarcinoma (10). Further, exposure to tamoxifen, a known inducer of liver cancer, increased hepatic miR-25 expression in rats (11). Notably, elevated miR-25 levels are not universally associated with a worse disease course, for instance in acute myelogenous leukemia (12). Therefore, the particular functional

Address for Correspondence: Justin L. Mott, MD, PhD Assistant Professor, University of Nebraska Medical Center, Department of Biochemistry and Molecular Biology, 985870 Nebraska Medical Center, Omaha, Nebraska, United States of America. justin.mott@unmc.edu.

effect of elevated microRNA quantities cannot necessarily be generalized from one tumor type to another.

Cholangiocarcinoma represents the second most common primary hepatobiliary cancer (13) and is resistant to apoptosis mediated by TRAIL, a major player in the extrinsic death pathway (14). Similar to other tumors, cholangiocarcinoma paradoxically expresses TRAIL (15-17) and, therefore, may rely on strong cellular survival signals for tumor development. We report a role for miR-25 in regulating apoptotic signaling in cholangiocarcinoma cell lines and human tumor samples. Increased miR-25 repressed Death Receptor-4 (DR4) protein expression protecting cells from TRAIL-induced death, and this effect was reversed on antagonism of miR-25.

MATERIALS and METHODS

Human Tissue Samples

All protocols involving patient materials were approved by the institutional review board, Mayo Clinic, Rochester MN. Cholangiocarcinoma samples from 15 patients and benign adjacent tissue from 4 patients were obtained intraoperatively and preserved according to a frozen tissue storage protocol. All samples were reviewed by a pathologist to verify the presence of malignant transformation.

Cell Culture

H69 is a non-malignant SV40-immortalized human cholangiocyte cell line, cultured as described (18). Malignant, patient-derived cholangiocarcinoma cell lines were: KMCH cells, derived from intrahepatic cholangiocellular-hepatocellular carcinoma, and Mz-ChA-1 cells, derived from metastatic gallbladder cancer. These were cultured in DMEM supplemented with 10% (v/v) heat-inactivated fetal calf serum, penicillin, streptomycin, and geneticin.

Manipulation of microRNA Levels

Consistent with current nomenclature (19), we refer to the mature sequences as 'miR' (as in miR-25; note capitalization), whereas clustered microRNAs, genes, and precursors are labelled 'mir' (as in mir-106b~25). pCDNA-mir-25 was constructed by amplification of 184 base pairs of human miR-25 and nearby sequence using the following primers: forward 5 '-TCTGGTCTCCCTCACAGGAC; reverse 5'-CATGGGTCGCCTACTCAC. After TOPO TA cloning (Invitrogen, Carlsbad, CA, USA), the SpeI/EcoRV fragment was subcloned into the XbaI/EcoRV sites of pCDNA3.1(+). *In vitro* transcription was performed (T7, Mega Script; Ambion, Austin, TX, USA) on linearized pCDNA-mir-25 or empty pCDNA3.1(+) as control. Antisense locked nucleic acids (LNA) were targeted to miR-25 or miR-106b, and compared to Negative Control A LNA (Exiqon, Vedbaek, Denmark). Cell lines were transiently transfected with microRNA precursor (final concentration, 7.5 nM) or antagonist (final concentration, 20 nM) with FuGENE HD (Promega, Madison, WI, USA) and Lipofectamine 2000 (Invitrogen) reagents, respectively. Total RNA was isolated 24 (precursor), or 48 hours (LNA) after transfection.

Quantitative Reverse Transcription Polymerase Chain Reaction

Total RNA was isolated using the mirVana kit (Ambion; for microRNA) or by Trizol (mRNA). MicroRNA was quantified by reverse transcription polymerase chain reaction (qRT-PCR; Applied Biosystems, Foster City, CA, USA). Profiling of 95 microRNAs plus RNU-6B was performed using Sybr Green detection and miScript primer assays (Qiagen, Valencia, CA, USA). mRNA quantitation was conducted utilizing Sybr Green-based detection technology (Roche Applied Science, Mannheim Germany). Primers for *DR4* (20), and 18S (21) have been described and for *MCM7* were: forward 5'-

TCTGGACATGAAGCTCATG; reverse 5'-GTAGTCAGCCAGAGACTCTG. For mRNA degradation studies, cells were treated for 0-6 hours with actinomycin D (5 μg/mL; Sigma) followed by *DR4* mRNA and 18S rRNA quantitation by qRT-PCR.

Apoptosis Studies

Recombinant human TRAIL from R&D Systems (375-TEC; Minneapolis, MN, USA) was used (1-5 ng/mL) to initiate apoptosis. Cells were analyzed via fluorescence microscopy for apoptotic nuclear morphology (condensation and fragmentation) after staining with 4'-6-diamidino-2-phenylindole (DAPI; Sigma, St. Louis, MO, USA). For apoptosis studies in cells transfected with miR-25-resistant *DR4*, green fluorescent protein (GFP)-tagged *DR4* (DR4-GFP)(22) was co-transfected with pCDNA-mir-25. Control studies included the GFP-N1 empty vector (Clontech, Mountain View, CA, USA). Only GFP-positive cells were scored for apoptotic nuclear morphology.

Immunoblotting

Whole cell lysates were obtained and processed for immunoblotting as described in detail previously (23). Primary antisera were: Death Receptor-4 (DR4; Alexis, San Diego, CA, USA), DR5 and c-FLIP (ProSci, Poway, CA, USA), Bim and caspase-8 (BD Biosciences, San Jose, CA, USA), Mcl-1 and actin (Santa Cruz Biotechnology, Santa Cruz, CA, USA: S19 for Mcl-1 and C-11 for actin).

Immunofluorescence

Cells cultured on collagen-coated glass coverslips were transfected and prepared for immunofluorescence analysis according to the protocol of Xu, *et al.* (24). Cells were incubated overnight with 1:1000 anti-DR4 (10 μg/mL) or anti-DR5 (5 μg/mL) antisera (ProSci), as indicated. Alexa Fluor® 488-labeled goat anti-rabbit IgG (Invitrogen), was diluted 1:2000 in blocking buffer. Cells were post-stained with DAPI and examined with confocal microscopy (LSM 510, Carl Zeiss, Jena, Germany), and images were analyzed using ImageJ (NIH, Bethesda, MD, USA). At least 23 cells were included in the analysis for each condition.

Luciferase Reporter Assay

MicroCosm (25) was used to predict the miR-25 binding site within *DR4*. The *DR4* 3'UTR was amplified from human genomic DNA using the following primers: forward 5'-GTCCTTGGGAGTGAAAGACTC; reverse 5'-GTAAAGACGGCATTTCACGATG. The 226 base-pair product was cloned (TOPO TA) and the SpeI/EcoRV fragment subcloned into the SpeI/NaeI sites of pMir-REPORT (Ambion). The resultant pMirDR4 was mutated by PCR using primers designed to incorporate a 2-base substitution into the miR-25 binding site (5'-CAGGTGTAGTGG converted to 5'-CAGGTGT**cc**TGG). The resulting pMirDR4 constructs were cotransfected with pRL-CMV (Promega). Twenty-four hours after transfection, firefly and *Renilla* luciferase activities were analyzed using the Dual-Luciferase Reporter Assay System (Promega). Protein content in lysates was measured using the Bradford method.

Statistical Analysis

At least three replicates were obtained for each condition in experiments with cell cultures. For quantitative continuous data differences between two groups, data were analyzed by Student's t-test with a threshold for significance defined at $p < 0.05$. When multiple comparisons were possible, ANOVA coupled with Bonferroni post hoc correction was used. For microRNA miScript evaluation, significance analysis of microarray (SAM) was applied. All data are presented as mean +/- standard error of the mean (SEM).

RESULTS

Hedgehog Signaling is Involved in Regulation of mir-106b~25 Expression

Activation of the Hedgehog signaling pathway is a recently appreciated feature of human cholangiocarcinoma (20, 26), with the potential to regulate microRNA expression (27). We sought to identify additional microRNAs that may be under control of Hedgehog signaling by profiling microRNA expression from KMCH cells that were untreated (vehicle), treated with the Smoothened inhibitor cyclopamine (5 μM), or treated with Sonic Hedgehog ligand (500 nM). Of the 95 microRNAs assayed, we determined that 14 microRNAs were downregulated upon Hedgehog inhibition (Table 1, and Supplemental Fig. 1). Of the cyclopamine-responsive microRNAs, miR-15b, miR-25, and miR-125a-5p were detected at the highest relative expression levels. Cyclopamine treatment decreased miR-15b expression by 52%, miR-25 by 76%, and miR-125a-5p by 51%.

We selected miR-25 for further analysis based on the magnitude of its repression upon cyclopamine treatment and its importance in tumor biology. Interestingly, miR-106b, which is part of the mir-106b~25 polycistron and located less than 600 bases from miR-25, was also significantly repressed by cyclopamine (Table 1). While miR-93, the third member of the mir-106b~25 cluster at this locus, was not identified by the statistical approach, a similar expression pattern of all three microRNAs is apparent (Fig. 1).

mir-106b~25 is Overexpressed in Cholangiocarcinoma

We next conducted studies to investigate if mir-106b~25 indeed is involved in cholangiocarcinoma biology. We first employed benign cholangiocytes (H69) and malignant cholangiocarcinoma (Mz-ChA-1, KMCH) cell lines. Quantitation of miR-106b, miR-93, and miR-25 expression demonstrated overexpression of all three microRNAs in cholangiocarcinoma cell lines compared with benign cells (Fig. 2A-C). Among 15 human primary cholangiocarcinoma tumor samples, 9 demonstrated an increase in miR-106b expression (Fig. 2D), a slight increase of miR-93 expression was demonstrated in four samples (Fig. 2E), and 6 samples exhibited increased miR-25 expression (Fig. 2F). Approximately 27% of human samples (4 of 15) had a concurrent increase of all three cluster members. Thus, mir-106b~25 expression is upregulated in malignant cholangiocarcinoma cell lines and a subset of primary cholangiocarcinomas.

To determine if increased expression of this cluster was due to elevated host gene RNA levels, we measured *MCM7* mRNA in H69, KMCH, and Mz-ChA-1 cells. There was significantly more *MCM7* in KMCH compared to H69 cells, while Mz-ChA-1 cells expressed similar amounts to H69 (Fig. 3A). In the primary human tumor samples, we analyzed 10 samples for *MCM7* mRNA levels, divided equally as 5 samples that had increased miR-25 levels (#69, 75, 29, 65, and 87) and 5 with low miR-25 levels (#85, 63, 73, 49, and 39). The amount of *MCM7* in the tumor samples that had high miR-25 was nearly 3-fold higher than those with low miR-25 (Fig. 3B). These data seem to indicate that increased host gene expression may explain, at least in part, the elevation of these microRNAs.

TRAIL-mediated Apoptosis is Attenuated by miR-25

To define the effect of miR-25 on apoptosis, we first employed the non-malignant H69 cells that had relatively lower miR-25 expression. Enforced expression of miR-25 protected these cells from TRAIL-induced apoptosis by >40% compared to control RNA (Fig. 4A). Next, we investigated the effect of miR-25 antagonism in KMCH cells, which normally express miR-25 at elevated levels. Upon antagonism of miR-25 with LNA-25, KMCH cells demonstrated at least a 25% increase in apoptosis compared to control-transfected cells (Fig.

4B). Therefore, we demonstrated that increased miR-25 protected, and, conversely, decreased miR-25 sensitized cholangiocarcinoma cell lines to TRAIL-induced apoptosis.

miR-25 Suppresses TRAIL Death Receptor

TRAIL Death Receptors DR4 and DR5, caspase-8, cellular FADD-like interleukin-1β – converting enzyme-inhibitory protein (c-FLIP), Mcl-1, and Bim all participate in the cell death pathway triggered in cholangiocarcinoma by TRAIL. Moreover, DR4, Bim, and Mcl-1 were identified by computational analysis as predicted targets for miR-25. We sought to identify the functional miR-25 targets that influence TRAIL signaling in cholangiocarcinoma. Quantitation of miR-25 expression after transfection with mir-25 precursor confirmed the overexpression paradigm (Fig. 5A). Similarly, antagonism of endogenous miR-25 was demonstrated in KMCH cells transfected with LNA targeting miR-25 (LNA-25; Fig. 5B). Cellular DR4, but not DR5, Bim, Mcl-1, Caspase-8, or c-FLIP protein expression was efficiently reduced by miR-25 overexpression in KMCH cells (Fig 5C). Because DR4 is a novel miR-25 target, we verified this interaction in H69 and Mz-ChA-1 cells (Fig. 5D). Conversely, antagonism of miR-25 caused increased DR4 protein expression in KMCH cells. Specificity of LNA-25 was confirmed by transfection of the miR-106b antagonist (LNA-106), which had no effect on DR4 protein levels (Fig. 5E). DR4 protein in each of these cell lines was readily detected, and found to be more abundant in Mz-ChA-1 cells (Fig. 5F).

Antagonism of miR-25 also increased DR4 protein levels when examined by immunofluorescence staining of KMCH cells. Specifically, cells transfected with LNA-25 demonstrated a significant increase in the intensity of DR4 immunostaining, an effect not seen for DR5 (Fig. 6A). Quantitation of the fluorescent signal revealed a greater than two-fold increase in DR4 immunoreactivity in LNA-25 transfected cells versus control LNA (CT; Fig. 6B). Conversely, upregulation of miR-25 in H69 cells resulted in significantly decreased DR4 immunoreactivity (Fig. 6C, 6D). This decrease is consistent with immunoblot data in H69 cells (Fig. 5D). These findings confirmed that DR4 is a target protein for regulation of the TRAIL-induced death pathway by miR-25.

Enforced DR4 Expression Restored TRAIL Sensitivity

H69 cells transfected with a miR-25 expression vector (pCDNA-mir-25) demonstrated resistance to TRAIL-induced apoptosis, as anticipated and consistent with Figure 4A above. Importantly, a *DR4* expression plasmid that lacked the *DR4* 3'UTR (and thus lacked the putative miR-25 binding site) lead to restoration of sensitivity to TRAIL-induced apoptosis in TRAIL treated cells (Fig. 6E). The effect of miR-25 to repress DR4 protein levels and protect cells from TRAIL-induced apoptosis is consistent with previous findings that DR4 is important in cholangiocarcinoma cells. Short-hairpin RNA against *DR4* protected KMCH cells from TRAIL-induced apoptosis, while transient transfection with a *DR4*-expression vector sensitized these cells to TRAIL (20).

Direct Targeting of DR4 *3'UTR by miR-25*

A proposed mechanism of microRNA regulation of protein expression is via binding of the microRNA to a region within a cognate mRNA, resulting in repression by either mRNA degradation or translational inhibition. The steady-state amount of *DR4* mRNA in H69, KMCH, and Mz-ChA-1 cells did not indicate that cell lines with elevated miR-25 (KMCH and MzChA-1) had depressed *DR4* mRNA levels (Fig. 7A). To further assess a potential inverse correlation, we measured *DR4* mRNA in patient-derived cholangiocarcinoma samples stratified into high (n = 5) or low (n = 5) miR-25. Again, elevated miR-25 was not strictly correlated with low *DR4* mRNA (Fig. 7B). Finally, increased miR-25 expression did not accelerate *DR4* mRNA degradation compared to control. Six hours after the addition of

the transcriptional inhibitor actinomycin D, miR-25 transfected H69 cells expressed 73.2% of *DR4* compared to time zero, while control cells expressed 44.1% (data not shown). Conversely, KMCH cells transfected with the miR-25 antagonist, LNA-25, showed only a slight increase in *DR4* mRNA stability, with *DR4* levels of 13.7% of time zero and control LNA-transfected cells had 7.1% of *DR4* after 6 hours of actinomycin treatment (now shown). Collectively, we interpret these data to support repression of DR4 protein expression through translational inhibition, rather than mRNA degradation.

To determine if the repression of DR4 is the result of direct binding to the *DR4* 3'UTR, we used a luciferase reporter assay employing the empty reporter (pMir), the reporter fused to the full-length *DR4* 3'UTR (pMirDR4), or the *DR4* reporter with a two-base mutation at the miR-25 binding site (pMirDR4-25mut; Fig. 7C). Compared to the parental vector, pMirDR4 exhibited inhibition of luciferase expression upon enforced miR-25 expression. Mutation of the miR-25 binding site partially mitigated repression (Fig. 7D). Therefore, our data are consistent with the hypothesis that miR-25 repressed DR4 protein levels via direct targeting of the 3'UTR of *DR4*.

DISCUSSION

We and others have begun to define the altered microRNA landscape in cholangiocarcinoma (28-32). The main findings of this project identified an important molecular mechanism of apoptosis regulation by the oncogenic miR-25. First, our study demonstrated that members of the mir-106b~25 cluster are upregulated in cholangiocarcinoma cell lines, KMCH and Mz-ChA-1, and a subset of human tumors. Second, we provided evidence that miR-25 serves as an antiapoptotic microRNA in these cells, protecting against TRAIL-induced apoptosis. Finally, we have identified a novel target of miR-25 in the extrinsic pathway of cell death, namely DR4. Antagonism of miR-25 caused increased DR4 protein expression and sensitized cells to apoptosis. Combined, these data support a functional role for elevated miR-25 expression in apoptosis regulation of cholangiocarcinoma. Each of these findings will be discussed below.

MicroRNA gene sequences are often located in clusters where multiple precursor sequences can be transcribed on the same primary transcript. A substantial portion of microRNA coding sequences lie within a host gene, commonly in an intron. For miR-25, both of these situations apply, as mir-106b~25 is in an intron of *MCM7*, located at the fragile site FRA7F on chromosome 7. Our data demonstrate increased expression of all three microRNAs from this locus in cholangiocarcinoma cells and some tumor samples. It is anticipated that transcription of this microRNA cluster is linked to that of the host gene, *MCM7*, as has been shown in other cell types (33, 34). Indeed, the current investigation revealed that miR-25 RNA and *MCM7* levels are correlated in H69 and KMCH (though not MzChA-1). Also, in tumor samples with high miR-25, *MCM7* was also elevated. These initial data may indicate that miR-25 is co-transcribed with the *MCM7* mRNA, however, additional contributions from altered processing and degradation cannot be ruled out.

The fact that some, but not all, human cholangiocarcinoma samples had increased miR-25 expression may indicate that a particular genetic predisposition, tumor microenvironment, or perhaps differences in underlying patho- or oncogenesis might determine miR-25 dysregulation. Hedgehog reactivation in cholangiocarcinoma and liver injury is emerging as an important pathologic signal (35). Interestingly, in a subset of medulloblastomas constitutive activation of Sonic Hedgehog was reported to be associated with overexpression of the microRNA cluster mir-17~92, a paralog of mir-106b~25 (36). We present initial findings consistent with stimulation of miR-106b, miR-93, and miR-25 by the oncogenic Hedgehog pathway. Interestingly, we did not observe an increase in microRNA expression

upon treatment with the recombinant Sonic Hedgehog ligand, which may indicate pre-existing pathway activation, for istance through autocrine expression of Hedgehog ligands (20). It is anticipated that additional signals may be discovered that also increase miR-25 levels in cholangiocarcinoma, possibly including host gene stimulation (37). Future studies may also investigate a potential link between clinical parameters (intrahepatic versus extrahepatic; localized versus advanced) and miR-25 expression.

Consistent with reports of other tumor types, we found that miR-25 had an antiapoptotic role in cholangiocarcinoma cells, specifically, by protecting from TRAIL-induced cell death. This observation was reinforced by experiments with a miR-25 antagonist, LNA-25, which lead to apoptosis stimulation in our study. Evasion of TRAIL-induced apoptosis would presumably exempt tumor cells from immunologic surveillance. As previously described, this death ligand is expressed in human cholangiocarcinoma samples, likely in response to interferon-γ within the tumor microenvironment (17). Thus, resistance to TRAIL-induced apoptosis observed in cholangiocarcinoma cell lines may be necessary for the establishment and maintenance of this cancer. Our data implicate a role for miR-25 overexpression in the resistance to apoptosis.

TRAIL apoptotic signaling in cholangiocarcinoma includes induction of the mitochondrial pathway of apoptosis. Mitochondrial dysfunction can be initiated by the BH3-containing protein Bim (38), and recently Bim was described as a target of miR-25 in esophageal neoplasia (34). Thus, we initially considered that miR-25 likely exerted its protective effect in cholangiocarcinoma cells through repression of Bim, thus decreasing the intracellular apoptotic signal. Surprisingly, we did not find that miR-25 suppressed Bim protein levels or that antagonism of miR-25 increased Bim expression in cholangiocarcinoma cells. We conclude that microRNA function is likely cell-type specific, and may be regulated by as yet unknown conditions.

Because Bim protein levels were not reduced by miR-25 (nor induced by LNA-25), we searched for alternate targets. The *DR4* mRNA has a predicted miR-25 binding site within the 3'UTR, and, indeed, experiments with miR-25 overexpression or inhibition induced reciprocal effects on DR4 protein levels. The repression of DR4 was specific, in that multiple other participants in the TRAIL death signaling pathway showed no change in response to miR-25 manipulation. Additionally, immunofluorescence studies of DR4 and DR5 demonstrated that only DR4 immunoreactivity was increased upon miR-25 antagonism. Finally, direct targeting of the *DR4* 3'UTR by miR-25 was identified by a luciferase reporter assay. Luciferase experiments demonstrated that miR-25 repression of the signal was dependent on the presence of the *DR4* 3'UTR, and mutation of the putative miR-25 binding site lead to restoration of luciferase expression. We note that this restoration may be partial, as careful inspection of the data reveals that the mutant construct displayed a slight decrease in signal upon enforced miR-25 expression, though this effect was not statistically significant. This observation might indicate the presence of additional, cryptic miR-25 binding sites.

DR4 protein expression includes several layers of regulation, e.g. epigenetic silencing, loss-of-function mutations, and dysregulation of cellular localization (39). Here we identified an additional mechanism controlling DR4 protein levels in cholangiocarcinoma cells, namely miR-25 repression of DR4. Possibly due to one or more of these alternative DR4 regulatory pathways, the DR4 protein signal in untreated cell lines *in vitro* is not inversely correlated with miR-25 expression. This lack of correlation cannot be taken as evidence that miR-25 does not regulate DR4, especially given the reciprocal effects of increased or decreased miR-25 on DR4 protein expression. We demonstrated that cells can be resensitized to

TRAIL-induced apoptosis upon restoration of DR4 protein in miR-25 transfected cells. It is likely that resting amounts of DR4 protein are determined by multiple mechanisms.

The finding that miR-25 targets DR4, coupled with the implication of Hedgehog as a mediator of increased miR-25 levels (Fig. 8) is consistent with the observation that Hedgehog inhibition both increased DR4 protein and sensitized to apoptosis (20). The findings reported in the previous work also demonstrated direct transcriptional repression of DR4, such that Hedgehog inhibition lead to increased *DR4* mRNA. This current manuscript builds on these observations, supporting a dynamic and complex inhibition of DR4 expression at the mRNA and protein levels.

In conclusion, overexpression of miR-25 in cholangiocarcinoma was observed to negatively regulate apoptosis signaling and DR4 protein levels. Thus, this microRNA may serve as an attractive candidate for suppression to facilitate increased tumor cell death during cytotoxic therapy of this and other cancers.

Supplementary Material

Refer to Web version on PubMed Central for supplementary material.

Acknowledgments

List of Abbreviations

|	
DAPI	4'-6-diamidino-2-phenylindole
DR4	Death Receptor-4
GFP	green fluorescent protein
LNA	locked nucleic acid
MCM7	minichromosome maintenance protein-7
qRT-PCR	quantitative reverse transcription polymerase chain reaction
SAM	significance analysis of microarray
SEM	standard error of the mean
TRAIL	TNF-related apoptosis inducing ligand
UTR	untranslated region

REFERENCES

1. Bartel DP. MicroRNAs: target recognition and regulatory functions. Cell. 2009; 136:215–233. [PubMed: 19167326]

2. Birks DK, Barton VN, Donson AM, Handler MH, Vibhakar R, Foreman NK. Survey of MicroRNA expression in pediatric brain tumors. Pediatric blood & cancer. 2011; 56:211–216. [PubMed: 21157891]

3. Poliseno L, Salmena L, Riccardi L, Fornari A, Song MS, Hobbs RM, Sportoletti P, et al. Identification of the miR-106b~25 microRNA cluster as a proto-oncogenic PTEN-targeting intron

that cooperates with its host gene MCM7 in transformation. Science signaling. 2010; 3:ra29. [PubMed: 20388916]

4. Petrocca F, Visone R, Onelli MR, Shah MH, Nicoloso MS, de Martino I, Iliopoulos D, et al. E2F1-regulated microRNAs impair TGFbeta-dependent cell-cycle arrest and apoptosis in gastric cancer. Cancer Cell. 2008; 13:272–286. [PubMed: 18328430]

5. Dacic S, Kelly L, Shuai Y, Nikiforova MN. miRNA expression profiling of lung adenocarcinomas: correlation with mutational status. Modern pathology : an official journal of the United States and Canadian Academy of Pathology, Inc. 2010; 23:1577–1582.

6. Meng F, Henson R, Wehbe-Janek H, Ghoshal K, Jacob ST, Patel T. MicroRNA-21 regulates expression of the PTEN tumor suppressor gene in human hepatocellular cancer. Gastroenterology. 2007; 133:647–658. [PubMed: 17681183]

7. Wong QW, Lung RW, Law PT, Lai PB, Chan KY, To KF, Wong N. MicroRNA-223 is commonly repressed in hepatocellular carcinoma and potentiates expression of Stathmin1. Gastroenterology. 2008; 135:257–269. [PubMed: 18555017]

8. Li W, Xie L, He X, Li J, Tu K, Wei L, Wu J, et al. Diagnostic and prognostic implications of microRNAs in human hepatocellular carcinoma. Int J Cancer. 2008; 123:1616–1622. [PubMed: 18649363]

9. Li Y, Tan W, Neo TW, Aung MO, Wasser S, Lim SG, Tan TM. Role of the miR-106b-25 microRNA cluster in hepatocellular carcinoma. Cancer Sci. 2009; 100:1234–1242. [PubMed: 19486339]

10. Chen L, Yan HX, Yang W, Hu L, Yu LX, Liu Q, Li L, et al. The role of microRNA expression pattern in human intrahepatic cholangiocarcinoma. J Hepatol. 2009; 50:358–369. [PubMed: 19070389]

11. Pogribny IP, Tryndyak VP, Boyko A, Rodriguez-Juarez R, Beland FA, Kovalchuk O. Induction of microRNAome deregulation in rat liver by long-term tamoxifen exposure. Mutat Res. 2007; 619:30–37. [PubMed: 17343880]

12. Wang Y, Li Z, He C, Wang D, Yuan X, Chen J, Jin J. MicroRNAs expression signatures are associated with lineage and survival in acute leukemias. Blood cells, molecules & diseases. 2010; 44:191–197.

13. Carriaga MT, Henson DE. Liver, gallbladder, extrahepatic bile ducts, and pancreas. Cancer. 1995; 75:171–190. [PubMed: 8000995]

14. Johnstone RW, Frew AJ, Smyth MJ. The TRAIL apoptotic pathway in cancer onset, progression and therapy. Nature Reviews Cancer. 2008; 8:782–798.

15. Ashkenazi A, Pai RC, Fong S, Leung S, Lawrence DA, Marsters SA, Blackie C, et al. Safety and antitumor activity of recombinant soluble Apo2 ligand. J Clin Invest. 1999; 104:155–162. [PubMed: 10411544]

16. Walczak H, Miller RE, Ariail K, Gliniak B, Griffith TS, Kubin M, Chin W, et al. Tumoricidal activity of tumor necrosis factor-related apoptosis-inducing ligand in vivo. Nat Med. 1999; 5:157–163. [PubMed: 9930862]

17. Ishimura N, Isomoto H, Bronk SF, Gores GJ. Trail induces cell migration and invasion in apoptosis-resistant cholangiocarcinoma cells. Am J Physiol Gastrointest Liver Physiol. 2006; 290:G129–136. [PubMed: 16166346]

18. Grubman SA, Perrone RD, Lee DW, Murray SL, Rogers LC, Wolkoff LI, Mulberg AE, et al. Regulation of intracellular pH by immortalized human intrahepatic biliary epithelial cell lines. Am J Physiol. 1994; 266:G1060–1070. [PubMed: 8023938]

19. Griffiths-Jones S, Grocock RJ, van Dongen S, Bateman A, Enright AJ. miRBase: microRNA sequences, targets and gene nomenclature. Nucleic Acids Res. 2006; 34:D140–144. [PubMed: 16381832]

20. Kurita S, Mott JL, Almada LL, Bronk SF, Werneburg NW, Sun SY, Roberts LR, et al. GLI3-dependent repression of DR4 mediates hedgehog antagonism of TRAIL-induced apoptosis. Oncogene. 2010; 29:4848–4858. [PubMed: 20562908]

21. Cazanave SC, Mott JL, Elmi NA, Bronk SF, Werneburg NW, Akazawa Y, Kahraman A, et al. JNK1-dependent PUMA expression contributes to hepatocyte lipoapoptosis. J Biol Chem. 2009; 284:26591–26602. [PubMed: 19638343]

22. Akazawa Y, Mott JL, Bronk SF, Werneburg NW, Kahraman A, Guicciardi ME, Meng XW, et al. Death receptor 5 internalization is required for lysosomal permeabilization by TRAIL in malignant liver cell lines. Gastroenterology. 2009; 136:2365–2376. e2361–2367. [PubMed: 19272388]

23. Guicciardi ME, Bronk SF, Werneburg NW, Yin XM, Gores GJ. Bid is upstream of lysosome-mediated caspase 2 activation in tumor necrosis factor alpha-induced hepatocyte apoptosis. Gastroenterology. 2005; 129:269–284. [PubMed: 16012953]

24. Xu L, Hui AY, Albanis E, Arthur MJ, O'Byrne SM, Blaner WS, Mukherjee P, et al. Human hepatic stellate cell lines, LX-1 and LX-2: new tools for analysis of hepatic fibrosis. Gut. 2005; 54:142–151. [PubMed: 15591520]

25. Griffiths-Jones S, Saini HK, van Dongen S, Enright AJ. miRBase: tools for microRNA genomics. Nucleic Acids Res. 2008; 36:D154–158. [PubMed: 17991681]

26. Berman DM, Karhadkar SS, Maitra A, Montes De Oca R, Gerstenblith MR, Briggs K, Parker AR, et al. Widespread requirement for Hedgehog ligand stimulation in growth of digestive tract tumours. Nature. 2003; 425:846–851. [PubMed: 14520411]

27. Mott JL, Kurita S, Cazanave SC, Bronk SF, Werneburg NW, Fernandez-Zapico ME. Transcriptional suppression of mir-29b-1/mir-29a promoter by c-Myc, hedgehog, and NF-kappaB. J Cell Biochem. 2010; 110:1155–1164. [PubMed: 20564213]

28. Selaru FM, Olaru AV, Kan T, David S, Cheng Y, Mori Y, Yang J, et al. MicroRNA-21 is overexpressed in human cholangiocarcinoma and regulates programmed cell death 4 and tissue inhibitor of metalloproteinase 3. Hepatology. 2009; 49:1595–1601. [PubMed: 19296468]

29. Braconi C, Huang N, Patel T. MicroRNA-dependent regulation of DNA methyltransferase-1 and tumor suppressor gene expression by interleukin-6 in human malignant cholangiocytes. Hepatology. 2010; 51:881–890. [PubMed: 20146264]

30. Kawahigashi Y, Mishima T, Mizuguchi Y, Arima Y, Yokomuro S, Kanda T, Ishibashi O, et al. MicroRNA profiling of human intrahepatic cholangiocarcinoma cell lines reveals biliary epithelial cell-specific microRNAs. J Nihon Med Sch. 2009; 76:188–197. [PubMed: 19755794]

31. Meng F, Henson R, Lang M, Wehbe H, Maheshwari S, Mendell JT, Jiang J, et al. Involvement of human micro-RNA in growth and response to chemotherapy in human cholangiocarcinoma cell lines. Gastroenterology. 2006; 130:2113–2129. [PubMed: 16762633]

32. Mott JL, Kobayashi S, Bronk SF, Gores GJ. mir-29 regulates Mcl-1 protein expression and apoptosis. Oncogene. 2007; 26:6133–6140. [PubMed: 17404574]

33. Poliseno L, Salmena L, Riccardi L, Fornari A, Song MS, Hobbs RM, Sportoletti P, et al. Identification of the miR-106b~25 microRNA cluster as a proto-oncogenic PTEN-targeting intron that cooperates with its host gene MCM7 in transformation. Sci Signal. 2010; 3:ra29. [PubMed: 20388916]

34. Kan T, Sato F, Ito T, Matsumura N, David S, Cheng Y, Agarwal R, et al. The miR-106b-25 polycistron, activated by genomic amplification, functions as an oncogene by suppressing p21 and Bim. Gastroenterology. 2009; 136:1689–1700. [PubMed: 19422085]

35. Omenetti A, Diehl AM. Hedgehog signaling in cholangiocytes. Curr Opin Gastroenterol. 2011; 27:268–275. [PubMed: 21423008]

36. Uziel T, Karginov FV, Xie S, Parker JS, Wang YD, Gajjar A, He L, et al. The miR-17~92 cluster collaborates with the Sonic Hedgehog pathway in medulloblastoma. Proc Natl Acad Sci U S A. 2009; 106:2812–2817. [PubMed: 19196975]

37. Kim DW, Kim JY, Moon JH, Kim KB, Kim TS, Hong SJ, Cheon YP, et al. Transcriptional induction of minichromosome maintenance protein 7 (Mcm7) in human cholangiocarcinoma cells treated with Clonorchis sinensis excretory-secretory products. Mol Biochem Parasitol. 2010; 173:10–16. [PubMed: 20236609]

38. Werneburg NW, Guicciardi ME, Bronk SF, Kaufmann SH, Gores GJ. Tumor necrosis factor-related apoptosis-inducing ligand activates a lysosomal pathway of apoptosis that is regulated by Bcl-2 proteins. J Biol Chem. 2007; 282:28960–28970. [PubMed: 17686764]

39. Mellier G, Huang S, Shenoy K, Pervaiz S. TRAILing death in cancer. Mol Aspects Med. 2010; 31:93–112. [PubMed: 19995571]
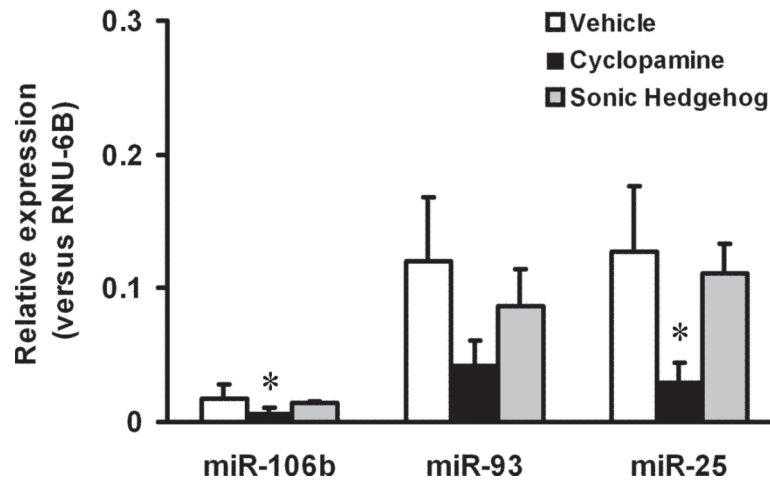
Figure 1. mir-106b~25 Expression is Supported by Hedgehog Signaling
Quantitation of mir-106b~25 expression in cholangiocarcinoma cells (KMCH) by qRTPCR
of total RNA isolated from cell lysates after 24 hr treatment with vehicle, sonic Hedgehog
(500 nM), or cyclopamine (5 μM). Expression of studied microRNAs was normalized to
RNU-U6 expression (delta-delta Ct). Mean +/- SEM, n = 3, miR-106b and miR-25
expressions were statistically different based on SAM analysis of Hedgehog versus
cyclopamine treatment groups, with a false discovery rate of zero.
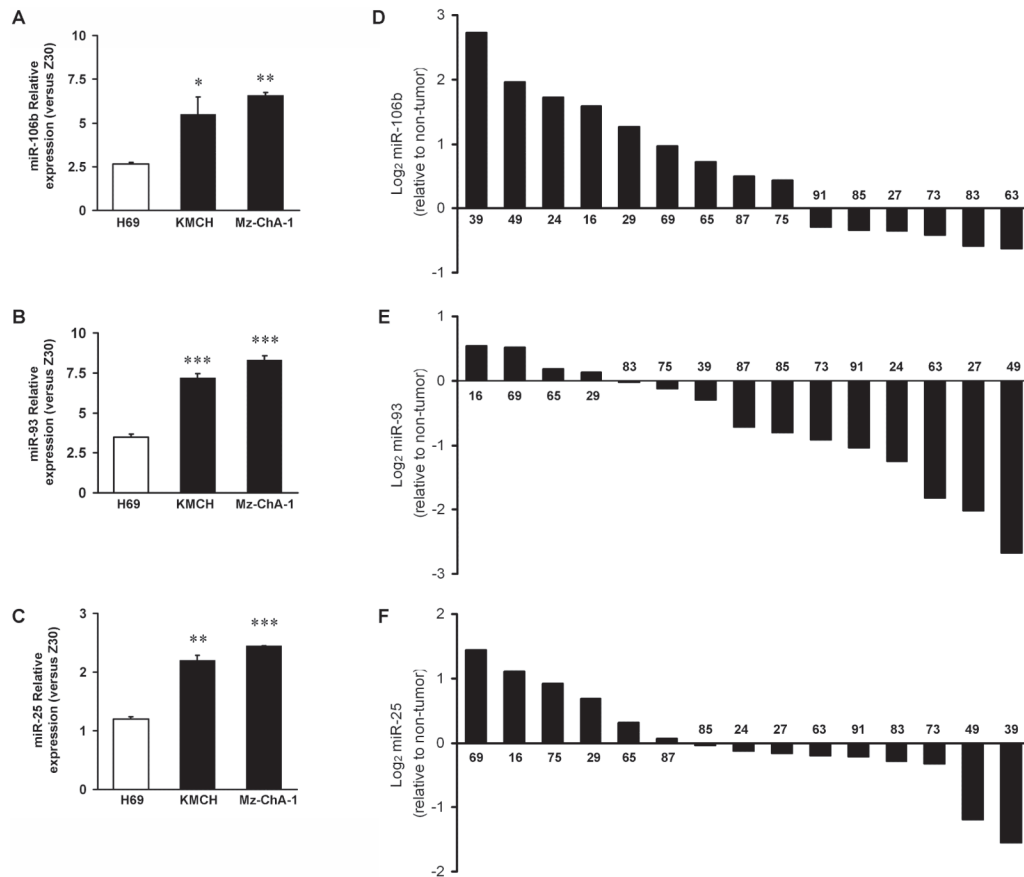
Figure 2. Increased Expression of mir-106b~25 in Cholangiocarcinoma Cell Lines and Human Tumor Samples

Panel A: miR-106b expression was measured by qRT-PCT from total RNA isolated from lysates of the indicated cell lines. Results are presented as relative expression using Z30 as an internal control and employing the delta-delta Ct method (mean +/- SEM; n = 3; *p < 0.05, **p < 0.01). Panel B: miR-93 expression from indicated cell lines, presented as above (***p<0.001). Panel C: miR-25 expression from the indicated cell lines, presented as above. Panel D: Similarly, miR-106b was measured by qRT-PCR of total RNA isolated from frozen human tumor samples. Relative expression was determined (delta-delta Ct) compared to Z30 (internal control) and results are presented as fold change (log_2) compared to the average expression measured in four non-malignant human liver samples, and sorted based on expression. Sample numbers indicate the patients from which each was obtained. Panel E: miR-93 expression from human tumor cells, presented as above. Panel F: miR-25 expression from human tumors, presented as above.
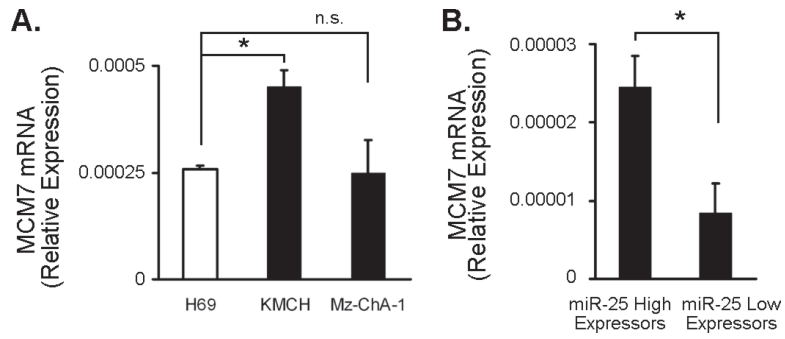
Figure 3. MCM7 mRNA Expression is Increased in Cholangiocarcinoma Cell Lines and Human Samples with High Expression of miR-25
Panel A: Quantitation by qRT-PCR of *MCM7* mRNA in whole cell lysates from non-malignant H69 cells compared to malignant KMCH and Mz-ChA-1 cells. Relative expression was determined (delta-delta Ct) compared to 18S (internal control), mean +/- SEM; n = 3; *p < 0.05. Panel B: *MCM7* mRNA levels were similarly quantified and analyzed in human cholangiocarcinoma samples comparing groups with high versus low miR-25 expression.
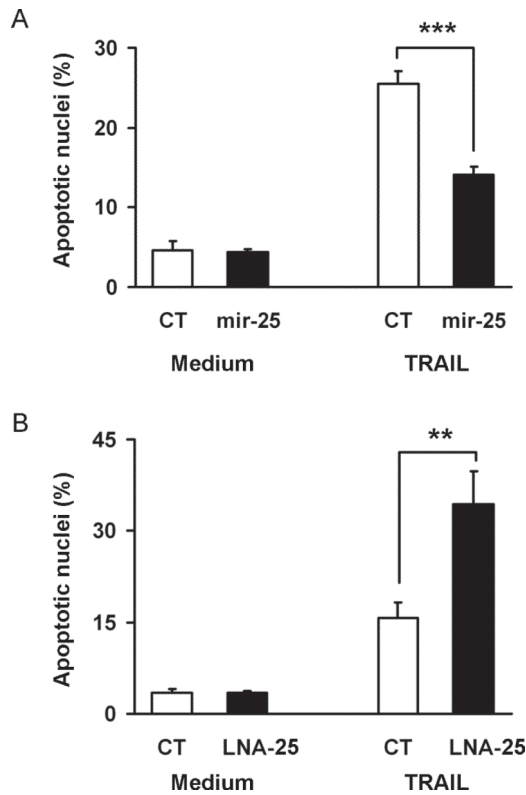
Figure 4. miR-25 Protects Cells from TRAIL-induced Apoptosis
Panel A: Non-malignant H69 cells were transfected with control RNA or mir-25 precursor as indicated to induce miR-25 overexpression. Eighteen hours after transfection, TRAIL was added at 4 ng/ml for an additional 6 hours to induce apoptosis. Cell were stained with DAPI and evaluated based on nuclear morphology for presence of apoptosis. Data are presented as the percentage of cells with apoptotic nuclear morphology out of total cell count and as mean of at least three experiments (mean +/-SEM, ***p<0.001). At least 100 cells were counted in each experiment. Panel B: In parallel, KMCH cells were transfected with control LNA (CT) or miR-25 antagonistic LNA (LNA-25). Two days after transfection, TRAIL at 4 ng/ml was added where indicated for an additional 6 hours. Cells were analyzed with DAPI for percent of apoptotic nuclei, as above (mean +/- SEM, **p<0.01).
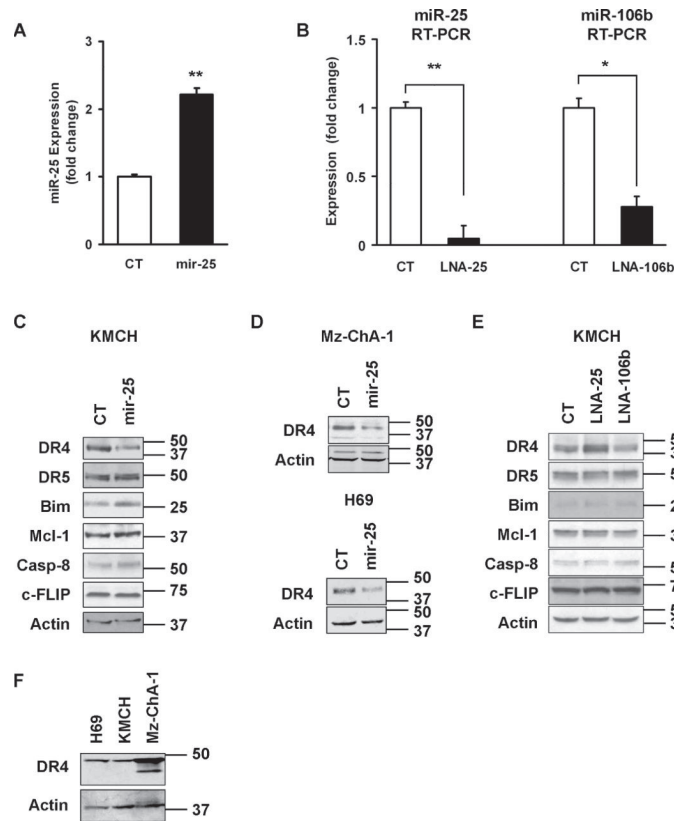
Figure 5. Altered miR-25 Reciprocally Affects DR4 Protein Expression
Panel A: KMCH cells were transfected with mir-25 precursor for 24 hours. Extracted total RNA was analyzed by qRT-PCR to confirm augmented miR-25 expression. Mean +/- SEM; n = 3, **p < 0.01. Panel B: KMCH cells were transfected (48 hr) with locked nucleic acid antagonists to miR-25 (LNA-25), miR-106b (LNA-106b), or control LNA (CT). Total RNA was then subjected to qRT-PCR for miR-25 (left) or miR-106b (right) as well as Z30 (internal control). Data are presented as relative expression (delta-delta Ct compared to Z30). Mean +/- SEM; n = 3, *p<0.05, **p<0.01. Panel C: KMCH total lysates were examined by immunoblot for the indicated polypeptides after cell transfection (24 hr) with control (CT) or mir-25 precursor. Actin was used as a loading control. Apparent molecular weight indicated in kilodaltons (kDa). Panel D: Similarly, Mz-ChA-1 or H69 cells were transfected with control or mir-25 precursor and total cellular protein was analyzed by immunoblot for DR4 and actin. Panel E: KMCH cells, where indicated, were transfected (48 hr) with control LNA (CT), LNA-25, or LNA 106b as a specificity control. Whole cell lysates were analyzed for the indicated polypeptides by immunoblot. Panel F: Total cellular protein was isolated from H69, KMCH, and Mz-ChA-1 cells and analyzed for DR4 protein by immunoblot with actin as a loading control.
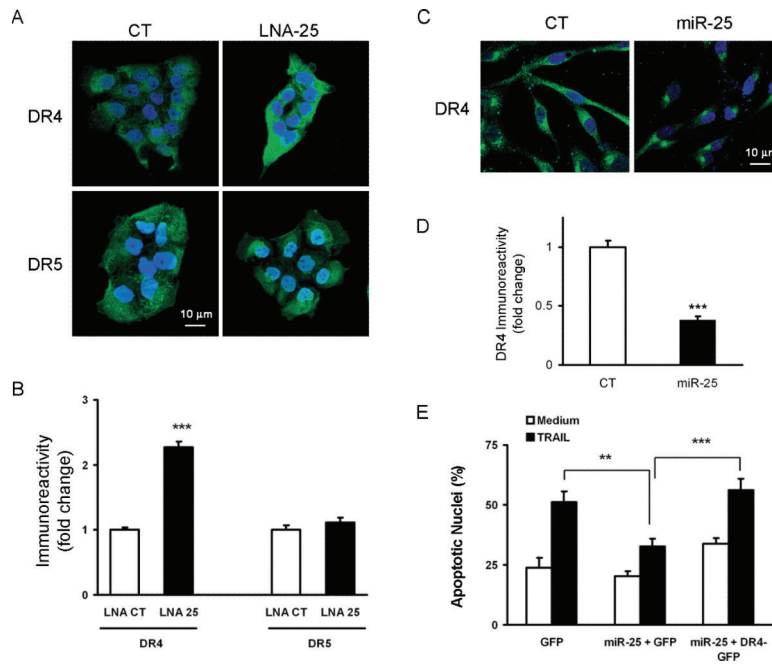
Figure 6. DR4 Repression by miR-25 and Functional Rescue Via miR-25-resistant DR4
Panel A: After transfection of KMCH cells with control locked nucleic acid (CT) or LNA
against miR-25 (LNA-25) for 48 hours, slides were prepared and analyzed by confocal
microscopy for immunofluorescence intensity of DR4 or DR5. Panel B: Fluorescence
intensity of cells transfected and stained as in panel A was quantified by ImageJ software.
The data are presented as fold change in the average DR4 or DR5 intensity, mean +/-SEM,
***p<0.001. Panel C: H69 cells were transfected (24hr) with control (CT) or mir-25
precursor; slides were prepared and examined for DR4 immunofluorescence by confocal
microscopy. Panel D: DR4 fluorescence intensity in H69 cells was quantified by ImageJ
software and presented as fold change in average signal intensity between control and
treatment groups, mean +/- SEM, ***p<0.001. Panel E: H69 cells were transfected with
GFP plus pCDNA, GFP plus pCDNA-mir-25, or DR4-GFP plus pCDNA-mir-25. Eighteen
hours after transfection, TRAIL was added at 4 ng/ml for additional 6 hours to induce
apoptosis. Cells were stained with DAPI and GFP-positive cells were evaluated based on
nuclear morphology for presence of apoptosis. Data are presented as the percentage of cells
with apoptotic nuclear morphology out of total cell count (mean +/-SEM, **p<0.01,
***p<0.001).
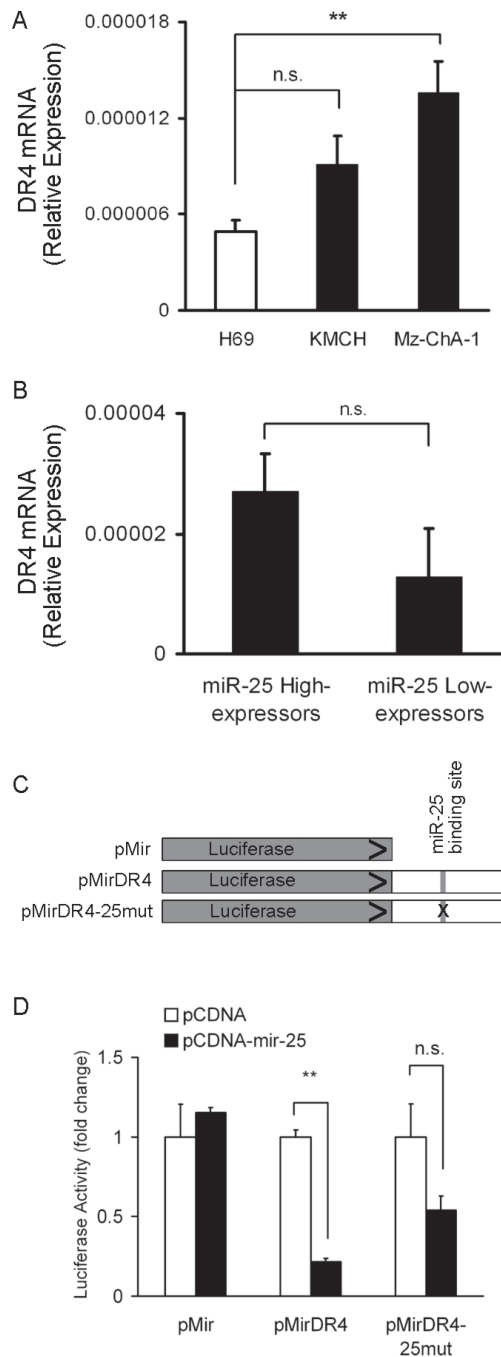
Figure 7. miR-25 Targets the *DR4* 3'UTR to Mediate Gene Expression
Panel A: Total RNA from H69, KMCH, and Mz-ChA-1 cell lines were analyzed for *DR4*
mRNA expression by qRT-PCR. Relative expression was determined (delta-delta Ct)
compared to 18S (internal control), mean +/- SEM; n = 3; *p < 0.05. Panel B: Human tumor
samples were grouped based on the level of miR-25 expression (high versus low) and
analyzed for *DR4* mRNA expression by qRT-PCR. Data are presented as relative expression
with 18S used as an internal control. Panel C: Schematic presentation of the empty parental
Luciferase reporter (pMir), the luciferase construct containing the full length *DR4* 3'UTR
(pMirDR4), and a two-base binding site mutant (pMirDR4-25mut). Panel D. KMCH cells
were transiently transfected with pMir, pMirDR4, or pMirDR4-25mut, as indicated. Cells

were also co-transfected with either empty control vector (pCDNA) or with a miR-25 expression vector (pCDNA-mir-25). Twenty-four hours after transfection, cells were lysed and luciferase activity measured. The activity was normalized to the total protein content, and expressed as fold change relative to the corresponding pCDNA value (set at 1.0), mean +/- SEM. ** $p < 0.01$; n.s. = not significant.
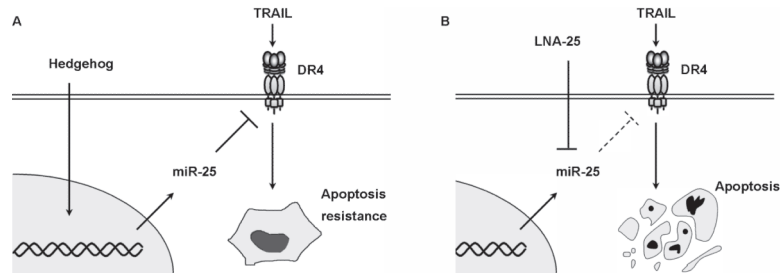
Figure 8. Regulation of Apoptosis by miR-25 Overexpression
Schematic diagram illustrating the role of miR-25 in cholangiocarcinoma TRAIL death-receptor signaling. Panel A. Increased miR-25 expression, driven in part by Hedgehog signaling, targets DR4 for repression which results in TRAIL resistance in tumor cells, permitting cell survival. Panel B. Antagonism of miR-25 via LNA-25 permits elevated DR4 protein levels, and thus increased tumor cell death.

Table 1

Cyclopamine suppression of microRNA expression

Inhibition of Hedgehog signaling (cyclopamine 5 μM for 24 hours) caused a reduction in microRNA expression for 14 microRNAs compared to cells treated with recombinant human Sonic Hedgehog. Data are presented as the percent reduction of the microRNA signal compared to Hedgehog-treated cells, such that no reduction would be reported as 0% and complete elimination would be 100% reduction. Only microRNAs with significant alteration (significance analysis of microarrays) are listed.

Gene Name	Reduction (%)
let-7g	74.27
let-7i	64.96
miR-15b	52.44
miR-22	54.28
miR-24	64.00
miR-25	76.43
miR-29c	55.98
miR-99a	34.93
miR-103	51.82
miR-106b	59.99
miR-125a-5p	51.32
miR-181b	41.71
miR-186	54.18
miR-191	39.47